INTERNATIONAL JOURNAL FOR NUMERICAL METHODS IN FLUIDS
Int. J. Numer. Meth. Fluids 2005; **47**:721–737
Published online 24 January 2005 in Wiley InterScience (www.interscience.wiley.com). DOI: 10.1002/fld.868

The challenge of turbulence modelling in modern aeronautical design

A. G. Hutton*,† and R. M. Ashworth

QinetiQ, Cody Technology Park, Ively Road, Farnborough, Hants, GU14 0LX, U.K.

SUMMARY

Modern aeronautical design is driven by a number of factors such as evolving operational requirements, the relentless drive to reduce costs and increasingly stringent environmental constraints. These have led to the requirement to treat a range of complex turbulent flow regimes. Designers demand a fine balance between simplicity of approach and competency, and thus research has inevitably focussed upon RANS-based turbulence modelling. This paper reviews the considerable progress of recent years in improving model proficiency for aerodynamic applications. The limitations to what can be achieved are discussed and it is suggested that some important flow regimes are beyond the RANS approach. The opportunities for the development and adoption of more advanced strategies such as hybrid RANS/LES methods are briefly examined. Copyright © 2005 John Wiley & Sons, Ltd.

KEY WORDS: aerodynamics; turbulence; RANS models; large eddy simulation; hybrid methods; detached eddy simulation

1. INTRODUCTION

Computational fluid dynamics (CFD) has been deployed successfully in aerodynamic design and assessment for a number of years. Indeed, the aeronautical industry has invested in the technology since the early days, with the result that it has now advanced to a considerable level of practical maturity. An aerodynamically well designed conventional surface is such that viscous effects are constrained to a thin boundary layer which stays attached to the surface together with a thin wake emanating from the trailing edge. The flow can then be addressed by solving the inviscid Euler equations, coupled to well calibrated semi-empirical treatments of the viscous layers. These methods, for which sophisticated turbulence modelling is clearly not an issue, have exerted an enormous impact on transonic wing design. However, in recent years the aspiration to treat complex viscous flow regimes has been growing rapidly. The

*Correspondence to: A. G. Hutton, QinetiQ, Cody Technology Park, Ively Road, GU14 0LX, Farnborough, U.K.
†E-mail: AGHUTTON@qinetiq.com

Contract/grant sponsor: Ministry of Defence; contract/grant number: C/EGCN02503E

Received 10 May 2004
Accepted 16 June 2004

principal motivation arises from the relentless drive to reduce operational costs and comply with ever more stringent environmental requirements which, in turn, lead to the emergence of novel design concepts.

The need for affordable, robust and competent treatments of complex turbulent flows is thus emerging as a pacing item in aerodynamic design. The starting point for devising such treatments is of course the compressible form of the Navier–Stokes and energy equations. These cannot be tackled directly (i.e. direct numerical simulation or DNS). At practical values of the Reynolds number, the range of length and time scales which must be calculated is far too vast. It has been estimated that the DNS of flow over a complete aircraft using a computer with teraflop performance would take several thousand years [1]. Clearly the effect of turbulence on the fluid dynamic parameters of interest must be modelled, and given that design practicalities dictate that calculations must take no more than a few hours on moderate computing resource, such models, with few exceptions, will be of the Reynolds-averaged Navier–Stokes (RANS) variety for the foreseeable future. It is now generally accepted that there is no universal statistical state of turbulence and hence no universal RANS model or even a single model which is competent across a broad class of flows.[‡] Consequently, models must be customized and calibrated to capture the flow physics of a given flow regime and its characterizing strain field. The clear objective is to balance greatest simplicity in formulation with competency. This paper first examines the complex turbulent flows which challenge current aerodynamic design and then reviews the considerable progress which has been made in recent years in improving model proficiency. The paper concludes by briefly exploring the limitations of RANS-based models and the opportunities for the development and adoption of more advanced strategies. The literature on turbulence modelling is voluminous and expanding rapidly. It is not possible in a short paper to address fully the evolution of the subject and instead, attention will concentrate on explaining those modelling developments which are influencing modern aerodynamic design practice. A more comprehensive exposition can be found in Reference [2].

2. THE IMPORTANCE OF TURBULENCE MODELLING TO AERODYNAMIC DESIGN

In the military field, modern operational requirements, such as the evolution of stealthy platforms and weapons systems, together with the drive to reduce costs are leading to designs featuring novel geometrical configurations and concepts which differ significantly from those which have previously evolved from optimizing aerodynamic performance. As illustrated by the following examples, these frequently feature complex flow regimes which are strongly influenced if not dominated by gross viscous effects. Modern platforms which are designed to minimize radar cross section give rise to wing shapes with unconventional leading and trailing edge angles of sweep as well as complex wing–body blendings. As a consequence, under normal operating conditions, the flow separates at the leading edge, leading to shear

[‡]This conclusion was formally endorsed by the participants in the Isaac Newton Institute Programme on Turbulence, Cambridge University, 1999–2000.

layer roll up and complex vortex dynamics and interactions. Strong shocks can occur on the upper surface precipitating boundary layer separation.

Engine intake ducts are compact and tend to be S-shaped in order to shelter the engine face from observation. This can cause 3d flow separation accompanied by vortex lift-off, subsequent re-attachment and pressure distortion at the engine face. It is important to be able to predict the pressure recovery and overall drag.

Stealth considerations preclude the external carriage of stores. These must be enclosed within the airframe and, as such, must be delivered through an aggressive aerodynamic environment when the bay is opened. Of particular concern is aero-acoustic resonance which results in discrete tones containing freestream levels of energy. This is driven by the complex interaction between the dynamics of the free shear layer and vortices shed from the lip of the cavity.

It is also desirable to eliminate dependence on deployable surfaces for aircraft control. Alternative flow control mechanisms such as those which change the lift distribution by activation of judicious local separation are therefore being explored.

In the civil field the quest for reduced cost of ownership and compliance with increasingly stringent environmental constraints largely drive modern design. Current concerns over noise during take-off and landing are stimulating efforts to reduce sound levels. For example, the demand on engine power can be reduced considerably by increasing the lift-to-drag ratio of the wing when it is set in low speed high lift configuration. Such design improvements are dependent upon the ability to model accurately complex interactions between boundary layers and wakes under conditions of strong adverse pressure gradients and streamline curvature. A considerable source of noise is the deployed undercarriage. In order to quantify the effect of design variations on this source it is necessary to simulate the turbulent structure in the wakes from the various components.

Much of the gains achievable in cruise drag reduction have been accomplished by optimizing wing design. Further incremental gains must be found by minimizing the effects of quite detailed and fairly complicated viscous flow regimes such as separated flow behind thick trailing edges, flow around wing tip devices and the interface between the powerplant installation and the wing. Finally, radically different aircraft concepts for increasing capacity at low cost are beginning to be explored. The knowledge base underpinning the design of such configurations will be generated using CFD rather than relying heavily on expensive and lengthy wind tunnel testing as in the past.

In summary, it is clear that turbulence modelling is increasingly being viewed as a pacing item in the development of competent aerodynamic design tools.

3. TURBULENCE MODELLING FOR THE RANS EQUATIONS

3.1. Introduction

The Reynolds stress terms in the RANS equations have to be closed before the equations can be solved. One option is to derive transport equations for these terms from the NS equations. Doing this introduces higher order correlations. Repeating the process for the higher order correlations introduces yet more correlations. The only way to form a closed set of equations is to model the correlations at some level. In practice this is done either at the level of the

Reynolds stresses themselves or at the next level of the Reynolds stress transport equations. The latter approach, known as Reynolds stress transport (RST) modelling, captures more of the physics but is more computationally intensive with 7 additional transport equations to solve. Given the desire to balance simplicity with competency, the former approach, represented by the various linear and non-linear eddy viscosity models, is the more practical approach for high Reynolds number applications.

3.2. Linear eddy viscosity models

Eddy viscosity models are founded on the Boussinesq hypothesis. This states that, by analogy with viscous stresses, the deviatoric part of the turbulent stresses are proportional to the strain of the mean flow through a dynamical eddy viscosity factor, μ_t, i.e. the Reynolds stresses, τ_{ij}, are given by

$$\tau_{ij} = -\langle \rho u_i' u_j' \rangle = \tfrac{2}{3}\rho k \delta_{ij} + \mu_\tau S_{ij} \tag{1}$$

where ρ is the density and k is the turbulent kinetic energy per unit mass. The instantaneous velocity components, u_i, has been divided as

$$u_i = U_i + u_i' \tag{2}$$

into a mean component, U_i and a fluctuation about the mean, u_i'. The brackets $\langle \ldots \rangle$, indicate taking the Reynolds (time) average of the enclosed quantity. The strain tensor for the mean flow is given by

$$S_{ij} = \frac{1}{2}\left(\frac{\partial U_i}{\partial x_j} + \frac{\partial U_j}{\partial x_i}\right) \tag{3}$$

For shear dominated flows in which normal stresses are unimportant, the task of the turbulence model is then to provide an appropriate turbulence velocity scale, V_t, and length scale L_t, from which to construct the eddy viscosity. The simplest (algebraic) models, which are applicable for thin attached shear layers, make use of local values of existing scales. These are the wall distance, which can be related to the maximum eddy size at this distance, and the product of wall distance with the mean shear, which can be related to the rotational velocity of these eddies. Models constructed in this way can perform well for surfaces designed to maintain thin shear layers throughout but fail badly for more challenging flow regimes such as those described in the preceding sections.

Flow subject to strong adverse pressure gradients leading to boundary layer thickening and separation require as a minimum that transport effects be introduced for the velocity scale in order to predict the behaviour up to separation. Any combination $V_t^m L_t^n$ $(m \neq 0)$ of the velocity and length scales will do equally well as a means of introducing these effects and one possibility is to consider the kinematic eddy viscosity, $\nu_t \equiv \mu_t/\rho \propto V_t L_t$. A very successful model of this type, the Spalart–Allmaras model [3], in fact involves an equation for a modified kinematic eddy viscosity, $\tilde{\nu}_t$. Thus,

$$\frac{D\rho\tilde{\nu}_t}{Dt} = c_{b1}\rho\tilde{S}\tilde{\nu}_t + \frac{1}{\sigma}\left[\nabla\cdot(\mu + \rho\tilde{\nu}_t\nabla\tilde{\nu}_t) + c_{b2}\rho(\nabla\tilde{\nu}_t)^2\right] - c_{\omega 1}\rho f_\omega\left[\frac{\tilde{\nu}_t}{d}\right]^2 \tag{4}$$

where c_{b1}, c_{b2}, $c_{\omega 1}$ and σ are model coefficients. f_ω is a function which decreases from one in the log layer to zero in the outer boundary layer and d is the wall distance. $\tilde{S}$ is given by

$$\tilde{S} = S + \frac{\tilde{\nu}_t}{\kappa^2 d^2} f_{v2} \tag{5}$$

with

$$f_{v2} = 1 - \frac{\chi}{1 + \chi f_{v_1}} \tag{6}$$

in which

$$\chi = \frac{\tilde{\nu}_t}{\nu_t} \tag{7}$$

and f_{v1} is a near wall damping function. S is based on the magnitude of the vorticity

$$S = \sqrt{2 W_{ij} W_{ij}} \tag{8}$$

where the vorticity tensor is given by

$$W_{ij} = \frac{1}{2}\left(\frac{\partial U_i}{\partial x_j} - \frac{\partial U_j}{\partial x_i}\right) \tag{9}$$

The actual dynamic eddy viscosity is then given by

$$\mu_t = \rho \tilde{\nu}_t f_{v1} \tag{10}$$

The Spalart–Allmaras model has been calibrated for use in aerodynamic flows and can work very well in these regimes up to separation. It will often perform even better than some of the more sophisticated models described below. However, in order to have any chance of predicting post-separation behaviour it is necessary to introduce transport effects for the length scale (wall distance is clearly no longer appropriate) and the Spalart–Allmaras model cannot be expected to perform well in separated regions. The minimum level of turbulence model that has any chance of achieving this is that of the two equations models.

Two equation models typically comprise an equation for the turbulent kinetic energy per unit mass, k, from which the turbulent velocity scale is obtained as $V_t = k^{1/2}$. The length scale determining equation can be formulated in terms of any quantity $V_t^m L_t^n$ for non-zero n. One choice has been the dissipation term, ε, that appears in the k equation. The resultant k–ε models have been widely used for many applications. However, they suffer some severe shortcomings which make them unattractive for aerodynamics applications. The k–ε models over respond to the application of adverse pressure gradients producing too large a shear stress and hence failing to predict separation. Huang and Bradshaw [4] conducted an analysis of log layer prediction under adverse pressure gradients for different choices, $V_t^m L_t^n$, of length scale variable. They found constraints on the choice of m and n which were not met by ε. However, these constraints were satisfied by another choice of variable, namely, the turbulence frequency, ω, with $m = 1$ and $n = -1$.

A turbulence model based on solving k–ω equations was first introduced by Wilcox [5]. There have since been a number of other k–ω based models designed to improve on that of Wilcox. The k–ω based models have found favour with the aerodynamics community because

of their widely demonstrated superior performance under adverse pressure gradients. In all the models the eddy viscosity is expressed in terms of k and the turbulence frequency ω as

$$\mu = \rho \frac{k}{\omega} \tag{11}$$

The k and ω variables are then obtained from solving modelled equations of the form

$$\frac{D\rho k}{Dt} = P_k + \frac{\partial}{\partial x_j}\left((\mu + \sigma_k \mu_t)\frac{\partial k}{\partial x_j}\right) - \rho\varepsilon$$

$$\frac{D\rho \omega}{Dt} = P_\omega + \frac{\partial}{\partial x_j}\left((\mu + \sigma_\omega \mu_t)\frac{\partial \omega}{\partial x_j}\right) - \beta\rho\omega^2 + C_D \tag{12}$$

where the production terms are given by

$$P_k = -\langle \rho u_i' u_j' \rangle \frac{\partial U_i}{\partial x_j}, \quad P_\omega = \alpha \frac{\omega}{k} P_k \tag{13}$$

with the Reynolds stresses $\langle \rho u_i' u_j' \rangle$ being given by Equation (1) and with α a model coefficient. In the diffusion terms, μ is the molecular dynamic viscosity and σ_k and σ_ω are turbulent diffusion coefficients. The dissipation term, ε, is given in terms of ω, k and model coefficient β^* by

$$\varepsilon = \beta^* \omega k \tag{14}$$

In the original k–ω model of Wilcox, there was no term corresponding to C_D (i.e. $C_D = 0$). This term was added in later models to overcome a particular limitation of Wilcox's model. It was found to be sensitive to the freestream value of the ω variable. Such a freestream sensitivity does not occur in the k–ε based models. The cross-diffusion term, C_D, is of the form

$$C_D \propto \frac{\rho}{\omega}\frac{\partial k}{\partial x_j}\frac{\partial \omega}{\partial x_j} \tag{15}$$

It acts at the edge of boundary layers to prevent the inwards diffusion of high levels of ω but is switched off in the log layer so as to retain the superior properties of the original Wilcox model in this region.

In Menter's baseline (BSL) model, [6], the benefits of k–w (log layer predictions under adverse pressure gradients) and k–ε (free-stream independence in the wake) are achieved by blending from the coefficients of the former near walls to the coefficients of the latter (formulated in k–ω variables) in the outer boundary layer. Thus the coefficients in this model are all of the form,

$$\phi = f_1 \phi_1 + (1 - f_1)\phi_2 \tag{16}$$

where ϕ_1 are coefficients corresponding to the k–ω model and ϕ_2 are coefficients corresponding to the k–ε model. The function, f_1, is designed so as to take a value close to one in the log layer and close to zero further out in the defect layer. The term C_D results from transforming the ε equation in to an equation for ω and has a coefficient in the BSL model which

is a blend between zero (its k–ω value) and its k–ε value. In Kok's turbulent/non-turbulent (TNT) model, [7], the coefficients are constant throughout the boundary layer but the cross diffusion term (15) is switched on only when it is positive.

Although the various k–ω models do perform better than the k–ε models under adverse pressure gradients they still do not perform as well as might be hoped. This can be understood in terms of their behaviour outside the log layer. A major difference between eddy viscosity models and the more general Reynolds stress transport models mentioned at the beginning of this section is that the latter can account for the transport of the principal shear stress. It has been observed by Bradshaw that under many experimental conditions the ratio of the shear stress to the turbulent kinetic energy is almost constant in the outer boundary layer region, e.g. for a principal shear stress $\tau = -\langle u_1', u_2' \rangle$

$$\frac{D\tau/k}{Dt} = 0 \tag{17}$$

whereas linear eddy viscosity models predict that

$$\frac{\tau}{k} = \rho\sqrt{\beta^* \frac{P_k}{\varepsilon}} = \rho\sqrt{\frac{P_k}{\omega k}} \tag{18}$$

This clearly does not remain constant along a streamline for which there is a departure from local equilibrium conditions ($P_k = \varepsilon$). Under strong adverse pressure gradients $P_k/\varepsilon \gg 1$ and Equation (18) results in an unduly large shear stress which inhibits separation. In reality the shear stress should respond more gradually in step with the turbulent kinetic energy itself rather than instantaneously as here.

In his shear stress transport (SST) model, [6], which is a development of his BSL model, Menter has sought to enforce the response given by Equation (17) without resorting to solving additional transport equations. Instead he makes use of an eddy viscosity limiter to prevent the shear stress exceeding the value given by Bradshaw's relation. Thus, for a simple shear flow $U(y)$, this is achieved by setting

$$\mu_t = \frac{\rho k}{\max(\omega; f_2 \beta^{*-1} \partial U/\partial y)} \tag{19}$$

This has been generalized to a tensorially invariant form

$$\mu_t = \frac{\rho k}{\max(\omega; f_2 \beta^{*-1} W)} \tag{20}$$

where W is the magnitude of the vorticity tensor as defined in (8) and (9). The factor f_2 is included in (19) and (20) to ensure the limiter is applied only for wall bounded flows where Bradshaw's relation holds, i.e. $f_2 \approx 1$ within boundary layers and $f_2 \approx 0$ elsewhere.

Menter's SST model has proved remarkably effective in predicting pressure induced separation from smooth surfaces and has become perhaps the most popular model currently in use amongst the aerodynamics community as well as with CFD users more generally. It's effectiveness is demonstrated in computations of flow over the axisymmetric bump of Bachalo and Johnson [8]. The model for this experiment consisted of an annular circular-arc bump (chord length $c = 0.2032\,\text{m}$, height $0.237\,c$) attached to a circular cylinder (radius $0.375\,c$) aligned with the flow direction. The flow accelerated to supersonic conditions over the first part of

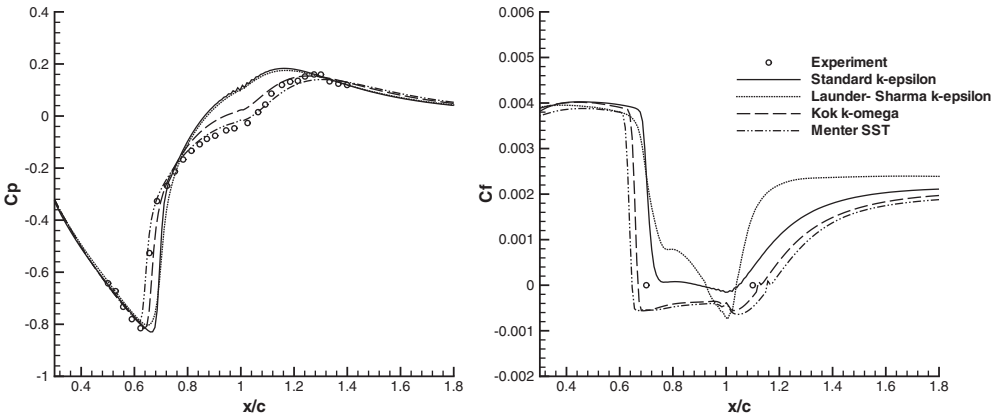

Figure 1. Surface pressure coefficient (left) and skin friction coefficient (right) for the Bachalo–Johnson axisymmetric bump in computations with two equation linear eddy viscosity models.

the bump, followed by a shock at a distance of about $x/c = 0.66$ from the bump leading edge. This led to a shock-induced separation at $x/c = 0.7$ and a reattachment downstream of the bump at $x/c = 1.1$.

The experiment formed one of the test cases of the VoTMATA collaboration reported in the paper of Hasan and McGuirk [9] and was computed with a wide range of turbulence models. The k–ε results from this work (generated by Loughborough University and UMIST) have been reproduced in Figure 1 together with some more recent k–ω based results (Kok and Menter SST models) from QinetiQ. As can be seen from the pressure distribution, the shock is located well downstream of the experimental location for both the high and low Reynolds number k–ε models and these models fail to predict the pressure plateau in the separation region indicating an insufficiently large recirculation region. The k–ω based models give a better prediction of the shock location and pressure plateau is better predicted (especially by the SST model).

From the skin friction distribution it is seen that the Menter SST model predicts a slightly early separation. The k–ε Kok model gives a separation location closer to the experiment while the k–ε models give a much delayed separation. This is consistent with the known poor performance mentioned earlier of k–ε models under conditions of strong adverse pressure gradient and the improvements that arise from using the ω scale determining equation.

Another interesting and desirable feature of the k–ω models compared to k–ε models is that they can be integrated through the near wall region of turbulent boundary layers without resorting to the use of arbitrary damping functions in the eddy viscosity and sources in the length scale determining equations. Such factors are essential for integration of k–ε models to the wall and can sometimes be the cause of numerical stiffness in the k–ε transport equations.

The absence, in particular, of eddy viscosity damping in k–ω models can be understood by Wilcox's suggestion that the k in his model is proportional to the wall normal component $\langle v'^2 \rangle$ of turbulent fluctuations. According to Townsend, near wall turbulence can be divided into an active vortical component arising in the inner layer which contributes to shear stresses and an inactive component arising from pressure fluctuations and large scale vortical structures in the outer layer which does not contribute. The k in the k–ω model corresponds only to the active

motion which is proportional to $\langle v'^2 \rangle$, and hence no eddy viscosity damping is required. The k in the k–ε model on the other hand, corresponds to the total kinetic energy (active plus inactive) and hence a damping factor is required to correct for the erroneous inclusion of the inactive component.

A more systematic attempt to obtain a velocity scale corresponding to the active turbulence was that of Durbin in his v^2–f model [10]. In addition to the undamped k–ε equations he solves an equation for $\langle v'^2 \rangle$. The latter has a source term, f, which is itself modelled through an elliptic relaxation equation. This is designed to introduce a wall blocking effect into the $\langle v'^2 \rangle$ equation. Use of $\langle v'^2 \rangle$ in place of k in the eddy viscosity then avoids the need for an eddy viscosity damping factor.

3.3. Non-linear models

For shear flows, linear eddy viscosity models enforce equality of the normal stresses. However, in some flows inequality of the normal stresses can be important. For example, in square duct flows this inequality drives secondary spanwise recirculations in each of the corners whilst linear models predict unidirectional flow. Linear models are clearly also not sensitized to rotational strains, i.e. they cannot distinguish between plane shear, plane strain and rotating shear. Attempts to remedy these deficiencies of the linear models have been directed towards non-linear extensions. There are many approaches to the derivation of non-linear models. One that has found favour in recent years is that of the explicit algebraic Reynolds stress models or EARSMs. These models are derived in a systematic fashion by applying simplifying assumptions to parent RST models. One of these assumptions, as shown below, is a generalization of Bradshaw's relation (17) between the turbulent shear stress and turbulent kinetic energy.

For the purpose of deriving EARSMs it is useful to consider the stress anisotropy tensor, b_{ij}, defined as the deviatoric part of the ratio of turbulent stress to turbulent kinetic energy,

$$b_{ij} = \frac{\langle u_i' u_j' \rangle}{2k} - \frac{1}{3}\delta_{ij} \tag{21}$$

In terms of the stress anisotropy the Reynolds stress transport equations for models with linear pressure strain correlations are of the form

$$\tau \frac{D\mathbf{b}}{Dt} = \frac{\tau}{2k}\left[\mathbf{D} - \left(\mathbf{b} + \frac{1}{3}\mathbf{I}\right)\{\mathbf{D}\}\right] - \frac{1}{a_4}\mathbf{b} - a_3\left(\mathbf{bS} + \mathbf{Sb} - \frac{2}{3}\{\mathbf{bSI}\}\right) + a_2(\mathbf{bW} - \mathbf{Wb}) - a_1\mathbf{S} \tag{22}$$

where boldface $\mathbf{T}$ is matrix vector notation for the corresponding second rank tensor T_{ij}, $\mathbf{I}$ is the identity tensor and $\{\mathbf{T}\}$ indicates the trace T_{ii}. The coefficients a_i are directly related to the pressure strain correlations used in closing the Reynolds stress transport equations. The tensor $\mathbf{D}$ represents the contributions from turbulent transport and viscous diffusion.

In order to derive a non-linear model from the RST equations it is necessary to make two simplifying assumptions. The first assumption is that

$$\mathbf{D} - \left(\mathbf{b} + \frac{1}{3}\mathbf{I}\right)\{\mathbf{D}\} \approx 0 \tag{23}$$

i.e. turbulent transport and viscous diffusion effects are negligible. The second assumption is a general form of Bradshaw's relation, namely that the turbulence is close to a *weak equilibrium* state in which stress anisotropy is invariant along streamlines

$$\frac{D\mathbf{b}}{Dt} \approx 0 \tag{24}$$

Substituting Equations (23) and (24) in (22) results in implicit algebraic equations for the anisotropy tensor. For general three-dimensional flows, the implicit equations can be made explicit (see Reference [11] for details) through the expansion of the anisotropy tensor in terms of 10 independent basis tensors. For two-dimensional flows only three of these basis tensors are independent and the expansion results in the following tensorially quadratic expression:

$$\mathbf{b} = -C_\mu \left[\mathbf{S} + a_1 a_4 (\mathbf{SW} - \mathbf{WS}) - 2a_3 a_4 \left(\mathbf{S}^2 - \frac{1}{3}\{\mathbf{S}^2\}\mathbf{I} \right) \right] \tag{25}$$

where

$$C_\mu = \frac{3a_1 a_4}{3 - 2a_3^2 a_4^2 \eta^2 + 6a_2^2 a_4^2 \xi^2} \tag{26}$$

and η and ξ are second invariants of strain and vorticity,

$$\eta = (S_{ij} S_{ij})^{1/2}$$
$$\xi = (W_{ij} W_{ij})^{1/2} \tag{27}$$

The full three-dimensional expression is much more complicated with terms that are tensorially quintic.

The coefficients a_i in the 2d model are all determined by constant coefficients in the pressure strain term of the underlying RST model except for a_4 which also depends on the ratio P_k/ε in the form

$$a_4 = \left(\gamma_0 \frac{P_k}{\varepsilon} + \gamma_1 \right)^{-1} \tag{28}$$

for constants coefficients γ_0 and γ_1. The ratio P_k/ε can be determined using

$$\frac{P_k}{\varepsilon} = -2\{\mathbf{bS}\} = 2C_\mu \eta^2 \tag{29}$$

Thus,

$$a_4 = (\gamma_1 + 2\gamma_0 C_\mu \eta^2)^{-1} \tag{30}$$

and Equations (26) and (30) require that C_μ be obtained by solving the cubic equation

$$\gamma_0^2 C_\mu^3 + \frac{\gamma_0 \gamma_1}{\eta^2} C_\mu^2 + \frac{1}{4\eta^4} \left[\gamma_1^2 - 2\gamma_0 a_1 \eta^2 - 2\eta^2 \left(\frac{a_3^2}{3} - a_2^2 \frac{\xi^2}{\eta^2} \right) \right] C_\mu - \frac{\gamma_1 a_1}{4\eta^4} = 0 \tag{31}$$

A similar analysis can be applied to the full 3d model but the algebra is much more complicated and such models are currently of little practical value. An exception is the 3d model

of Wallin and Johansson [13], which is based on the pressure strain model of Launder *et al.* [14]. In this model the coefficient a_3 in Equation (22) is small and the corresponding term is neglected. This simplifies the model considerably with only 5 of the 10 basis tensors having non-zero coefficients. The counterpart of Equation (31) is sixth-order and is not solved exactly. Instead an approximate solution to the equation is given.

4. LIMITATIONS OF RANS

Flow recovery following reattachment appears consistently to be poorly predicted by even the most sophisticated RANS turbulence models. Invariably, RANS computations display a less rapid recovery of the reattaching boundary layer than seen in the experiment. This arises from an underprediction of eddy viscosity (stress/strain) levels in the inner boundary layer with consequent reduced transfer of momentum towards the surface (see, e.g. Reference [15]).

In their experimental investigation Castro and Epik [16] have shown that it is structures in the outer boundary layer, formed in the mixing layer prior to reattachment, that control the development of the boundary layer. These structures only very gradually evolve into the type of structures more typically seen in canonical boundary layers. Development of the inner layer appears to follow from that of the outer layer. However, in RANS computations development of the inner layer is governed by the proximity of the wall with little influence of the outer layer. Existing models based on a single turbulence length scale are unable to capture the control of inner layer development by turbulent structures in the outer layer.

This limitation of RANS with respect to capturing flow recovery is well illustrated by the asymmetric diffuser experiment performed first by Obi *et al.* [17] and subsequently by Buice and Eaton [18]. Fully developed channel flow (height H) enters the diffuser with upper wall inclined upwards at 10°. Exit from the diffuser is into a channel of height $4.7H$. Strong adverse pressure gradients in the diffuser cause the flow to separate from the upper wall with subsequent reattachment on the exit channel upper wall. Data from the Buice–Eaton experiment includes velocity and stress profiles in the exit channel including the recovery region. This experiment was one of the test cases in the 8th ERCOFTAC/IAHR/COST workshop on refined turbulence modelling [19]. Results taken from the workshop illustrate the limitations of RANS computations. Figure 2 shows velocity profiles immediately after the experimental reattachment point and much further downstream in the recovery region. As can be seen, the velocity profile well downstream of reattachment continues to display the asymmetry seen at reattachment (particularly in the case of the Menter SST model) whilst the experimental profile is almost symmetric by this point. This is consistent with higher eddy viscosity (stress/strain) levels in the experiment.

5. BEYOND RANS

It would seem that there are important flow regimes which are beyond the competency of statistical RANS-based models (or at least any model which has not yet been devised). Chief amongst these are post-separated flow, particularly flow recovery following reattachment, and complex vortical-shear layer interactions. For these flow regimes, amongst others, alternative, practically viable strategies must be sought. As already stated, direct simulation across all

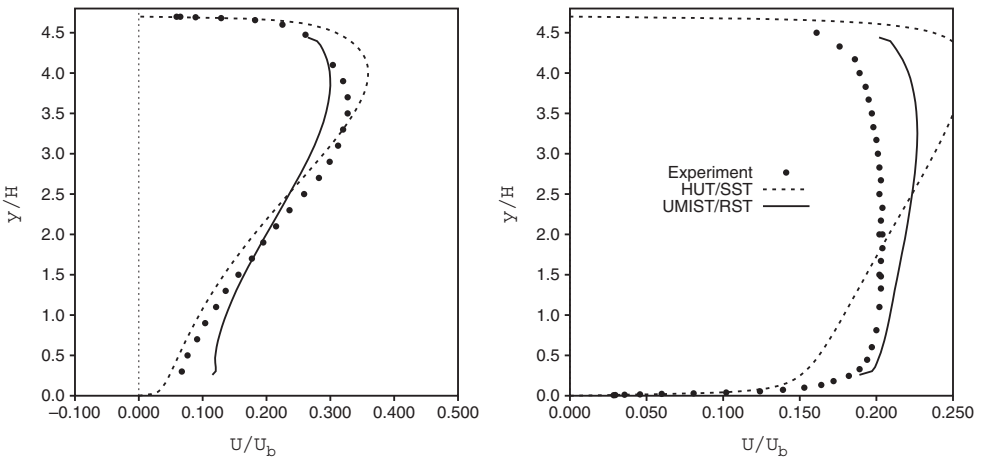

Figure 2. Velocity profiles in the asymmetric diffuser experiment of Buice and Eaton computed with Menter's SST model and the Gibson–Launder high Reynolds number RST model with wall functions. On the left, profiles just after reattachment ($x/H = 30.48$) and on the right, profiles following flow recovery ($x/H = 53.39$). Plots extracted from those in 8th ERCOFTAC/IAHR/COST workshop on refined turbulence modelling with editor's permission.

turbulent scales is not feasible at engineering values of the Reynolds number (Re). The ratio of the largest to smallest eddy size is proportional to $Re_t^{3/4}$, where Re_t denotes the turbulence Reynolds number. Thus, the computational cost of direct simulation scales approximately as the cube of Re. Fortunately, for fully developed turbulence, it is only the larger eddies, across which most of the energy is distributed, which play a significant role in determining the all important Reynolds stresses. This provides the rational for large eddy simulation (LES) in which the dynamics of the large eddies is calculated and that of the small eddies is modelled. Recent advances in computer power have rendered this approach feasible in many engineering applications. The LES literature is vast and many flavours have and continue to be developed. Thus, only a brief explanation of those which have found their way into practice is possible here. A more comprehensive account can be gleaned by consulting [20–22].

The key to the approach is the introduction of a low-pass spatial filter which when applied to a dependent flow variable separates the resolved from the unresolved elements of that variable. Thus, the filtered velocity components, $\bar{u}_i$ are defined as

$$\bar{u}_i(\underline{x}, t) = \int u_i(\underline{x}', t) G(\underline{x} - \underline{x}'; \Delta)\, \mathrm{d}\underline{x}' \tag{32}$$

where the filter kernel, G, includes a filter width Δ in its definition. Scales greater than Δ are explicitly resolved whilst those smaller than Δ are modelled. Commonly adopted filters use top-hat or Gaussian kernels. When each term in the Navier–Stokes equations is operated on by the filter, the original form of the equations is returned but with the dependent variables replaced by their filtered counterparts, plus the appearance of an additional term, $-\partial\tau_{ij}/\partial x_j$, on the right-hand side of the momentum equations. The stress tensor $\tau_{ij} = \overline{u_i u_j} - \bar{u}_i \bar{u}_j$ arises from the action of the unresolved dynamics and must be modelled in terms of the filtered variables. One of the simplest and historically one of the most commonly used models is the

Smagorinsky model. This employs the notion of a sub-scale eddy viscosity, ν_t, by which

$$\tau_{ij} - \tfrac{1}{3}\tau_{kk}\delta_{ij} = -2\nu_t\overline{S}_{ij} \tag{33}$$

where $\overline{S}_{ij}$ is the filtered velocity rate-of-strain tensor and τ_{kk} can be conveniently absorbed into the filtered pressure. The closure is completed by relating ν_t to Δ and $|\overline{S}| \equiv \sqrt{2\overline{S}_{ij}\overline{S}_{ij}}$

$$\nu_t = C_S^2\Delta^2|\overline{S}| \tag{34}$$

where C_S is the Smagorinsky constant which is usually set to the value of 0.1. For a fixed value of the filter width, Δ, progressive grid refinement will, in principle, result in convergence to the solution of the LES equations. In practice this would require a large value of Δ/h, where h is the grid size, so that on affordable grids the range of resolved scales is much reduced. Thus, Δ/h is usually set to a fixed value, typically unity, so that as the grid is refined more of the fine scale structure is resolved.[§] The stresses, τ_{ij} are then termed the sub-grid stresses (SGS). Under this strategy, the sub-grid physical model changes with grid-refinement and this leads inevitably in an interaction between modelled physics and numerical error, which is difficult to disentangle. Numerical effects must be treated with great care if spurious results are to be avoided. It is generally recommended that dissipative (i.e. upwind) schemes are avoided and that smoothly varying, near-orthogonal grids are adopted [23]. The Smagorinsky model can be applied close to a wall only if suitable damping functions are introduced to reduce ν_t in an appropriate way as the wall is approached. Alternatively wall functions can be devised to bridge the wall near region of flow [21].

In complex, non-homogeneous flows it is optimistic to expect a single calibrated value for C_S to suffice at all points in space and time. It is therefore usual to adopt dynamic formulations of the sub-grid model by which the filtered variables are subjected to a second filtering operation, called the test filter, using a larger filter width $\tilde{\Delta}$. Let $\sim$ above a variable denote the operation of the test filter. Then the Germano identity states that

$$L_{ij} = \widetilde{\overline{u}_i\overline{u}_j} - \tilde{\overline{u}}_i\tilde{\overline{u}}_j = \tau_{ij}^* - \tilde{\tau}_{ij} \tag{35}$$

where $\tau_{ij}^* = \widetilde{\overline{u}_i\overline{u}_j} - \tilde{\overline{u}}_i\tilde{\overline{u}}_j$ is the secondary stress tensor which arises when the LES equations themselves (i.e. the equations in terms of $\overline{u}_i$, etc.) are operated upon by the test filter. It is clear that L_{ij} can be calculated directly by test filtering the filtered velocities. This permits the Smagorinsky constant to be implicitly determined. If M_{ij} is defined such that $L_{ij} = C_S^2 M_{ij}$ then, on interpreting the stresses on the right-hand side of Equation (35) with the Smagorinsky model

$$M_{ij} = -2\left(\tilde{\Delta}^2\left|\tilde{\overline{S}}\right|\tilde{\overline{S}}_{ij} - \Delta^2\widetilde{|\overline{S}|\overline{S}_{ij}}\right) \tag{36}$$

The value of C_S is usually constructed by minimizing $\varepsilon = (L_{ij} - C_S^2 M_{ij})$ in an average sense over a local region of space and the test filter width is usually chosen as 2Δ. One of the advantages of the dynamic formulation is that it can be applied in near wall regions without modification. A number of other SGS modelling strategies have been proposed, such as mixed

[§]The adoption of a variable filter width implies that the filter and differentiation operators no longer commute and so the LES equations used in practice are not able to be formally derived from the Navier–Stokes equations.

models which combine two different approaches, the tensor eddy viscosity model, one equation models, and inverse modelling by which sub-filter stresses are inferred by approximate deconvolution. Further details can be found in References [20–22]. A controversial branch of research is monotonically integrated LES or MILES [24] which is based upon the observation that high-resolution numerical methods applied directly to the Navier–Stokes equations (*viz*. non-linear, second-order monotonic schemes) seem to mimic the properties of a SGS model. Thus, the model is implied by the numerical treatment and is not introduced explicitly.

Unfortunately, from the practical viewpoint, LES has not proved very successful in analysing the more challenging of aerodynamic flows such as those featuring smooth surface separation. It transpires that the turbulent structures adjacent to the wall must be fairly well resolved thereby obviating the use of wall functions. These structures have dimensions Δx^+, Δy^+, Δz^+ typically of order 100, 10, 20, respectively. This together with the above-mentioned requirement for smoothly varying, near-orthogonal grids makes huge demands on computational cost. The recent European collaborative project, LESFOIL, used LES to analyse flow over the Aerospatiale A-aerofoil at an angle of incidence of 13.3° and chord *Re* of 2.1 million [25]. In order to obtain good results, grids of up to 18 million points were required and even then these covered only 1.2% chord in the spanwise extent. Realistic design configurations are clearly beyond analysis. Spalart has estimated that LES of an airliner wing will not become a practical proposition for the next four decades [26].

In an attempt to circumvent this difficulty, considerable effort is being invested in the development and demonstration of RANS/LES hybrid methods. According to this approach, the layer of fluid near the wall is treated with (unsteady) RANS, whereas LES is used in the wall-remote region. The rationale is that modern RANS models perform quite well in attached wall layers up to the point of separation and their use avoids the intense grid resolution demanded of LES. Of course, difficult questions remain to be answered such as where should the RANS/LES interface be located and how should spectral information be handled across the interface (i.e. the seeding of LES from RANS level of information and the reverse process). Nonetheless, some important results have been obtained. Using a one-equation RANS model and a separate one-equation SGS model, Dahlstrom and Davidson have calculated the post re-attachment recovery of the velocity field in the Buice–Eaton asymmetric diffuser with reasonable accuracy [27].

One particular genre of hybrid method has attracted considerable attention in recent years. This is the detached eddy simulation (DES) method first introduced by Spalart and his co-workers in 1997 [26]. They propose that the length scale d in the destruction term of the Spalart and Allmaras RANS model (Equation (4)) is replaced by $d = \min(d, C_{\mathrm{DES}}\Delta)$, where Δ is the largest of the mesh spacing taken across all three co-ordinate directions at the point in question and C_{DES} is a model constant. Within a boundary layer, close to a wall, d is fairly small and due to the anisotropic nature of the mesh, featuring cells with very high aspect ratios, Δ is comparatively large, and thus the model selects the RANS option. Further away from the wall and especially in the regions of the mesh designed to capture separated flow, the grid cells are more isotropic and $\Delta < d$. The model then acts as a one-equation SGS model and LES ensues. Indeed, if transport terms are ignored in Equation (4), then with d set to $C_{\mathrm{DES}}\Delta$, the expression for ν_t is similar to Smagorinsky. DES is difficult to set up in complex configurations and success is crucially dependent on getting the mesh design right [28]. Indeed, the mesh design can be considered as a key element of the turbulence model. It is also not clear how precisely the information flow between the RANS and LES regions is

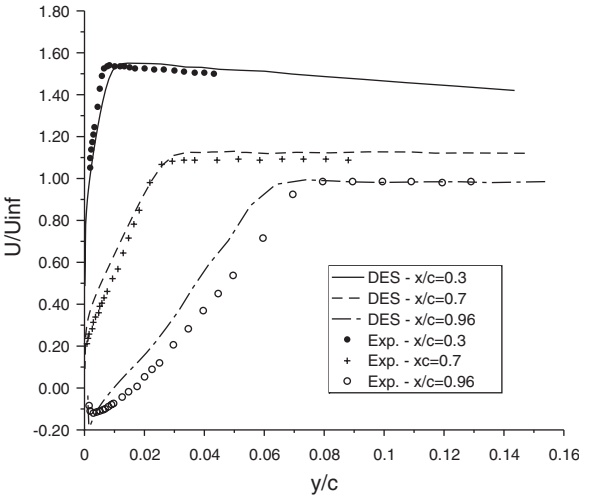

Figure 3. DES of Aerospatial A aerofoil by Cokljat and Liu (courtesy of Fluent).

handled. In addition, the dissipative upwind schemes normally used for RANS analysis must be blended with central based schemes operating in the LES region. Despite these drawbacks, some impressive DES applications have appeared in the literature. Within the LESFOIL consortium Cokljat and Liu [29] applied DES to the aerofoil problem and were able to produce fairly good results on grids of less than 4×10^5 cells (see Figure 3).

In principle, DES can be adapted to work with other RANS formulations, such as the Menter model [30]. From Equations (21) and (14), the destruction term in the modelled k-equation is $-\beta^* \rho k \omega \equiv -\rho k^{3/2}/L_t$ where the turbulent length scale $L_t = k^{1/2}/(\beta^* \omega)$. The DES adaptation now proceeds by simply multiplying the destruction term by f_{DES} where,

$$f_{\mathrm{DES}} = \max\left(\frac{L_t}{C_{\mathrm{DES}}\Delta}, 1\right) \tag{37}$$

and C_{DES} is set to 0.78. As discussed above, close to a wall L_t is typically less than $C_{\mathrm{DES}}\Delta$ due to high cell aspect ratios and then the unadulterated RANS model prevails. However, with suitable mesh design the opposite is true in the region where LES is desired and the destruction term is then changed to $\rho k^{3/2}/(C_{\mathrm{DES}}\Delta)$. That is, the length scale is reduced to $C_{\mathrm{DES}}\Delta$, stimulating the initiation of LES. One of the potential pitfalls of DES is that if the cell aspect ratio close to the wall is reduced significantly in order to capture a local feature, such as a shock or geometrical detail, the turbulence model may well switch inappropriately to LES-mode precipitating premature separation. In order to avoid such occurrences, Menter [31] advocates forcing f_{DES} to be unity whenever the $f1$ blending function in his model (Equation (16)) is also unity. This is done by multiplying $L_t/(C_{\mathrm{DES}}\Delta)$ in Equation (37) by $(1 - f_1)$.

Hybrid methods such as DES provide a very active and fruitful area of research and the current indications are that they will mature in the not too distant future into affordable and competent methods of analysis for a broad range of challenging flows.

6. CONCLUSIONS

The requirement to treat a range of complex turbulent flow regimes is a pacing item for modern aerodynamic design. Direct numerical simulation (DNS) of these regimes through solution of the Navier–Stokes equations is far beyond affordable computing capabilities for many decades to come. Thus turbulence modelling is imperative. The practical considerations of the design environment dictate that the simplest level of modelling is employed which meets competency criteria for the particular flow regimes encountered. Inevitably then, the focus of research has been on RANS-based models. Considerable progress has been made in recent years and a number of traditional modelling approaches have been superseded by a hierarchy of practical variants of increasing sophistication. Much is now known about their capabilities and limitations enabling the designer to select the most appropriate for his design purpose.

Certain flows seem to be beyond the competency of RANS modelling, or at least any model yet devised (e.g. recovery post separation and reattachment, complex vortical-shear layer interactions). For these it is fruitful to resolve the larger unsteady energy containing structures in the turbulence cascade. LES is designed to do this but cannot be practically applied in near wall regions due to excessive resolution requirements. Hybrid approaches are now being developed which combine RANS in near wall regions with LES in unsteady regions. With further advances in computing power this approach could emerge as a practical design tool in the near future but much further work is still required to mature the basic methodology.

ACKNOWLEDGEMENTS

This paper was written as part of a project funded under the MoD's corporate research programme.

REFERENCES

1. Moin P, Kim J. Tackling turbulence with supercomputers. *Scientific American* 1997; **276**:62–68.
2. Leschziner MA, Drikakis D. Turbulence modelling and turbulent flow computation in aeronautics. *The Aeronautical Journal* 2002; **106**:349–384.
3. Spalart PR, Allmaras SR. A one-equation turbulence model for aerodynamic flows. *AIAA Paper 92-0439*, 1992.
4. Huang PG, Bradshaw P. The law of the wall for turbulent flows in pressure gradients. *AIAA Journal* 1995; **33**(4):624–632.
5. Wilcox DC. Reassessment of the scale-determining equation for advanced turbulence models. *AIAA Journal* 1988; **26**(11):1299–1310.
6. Menter FR. Zonal two-equation k-turbulence model for aerodynamic flows. *AIAA Paper 93-2906*, 1993.
7. Kok JC. Resolving the dependence on free-stream values for the k-omega turbulence model. *NLR-TP-99295*, 1999.
8. Bachalo WD, Johnson DA. Transonic turbulent boundary layer separation generated by an axi-symmetric flow model. *AIAA Journal* 1991; **24**(3):437–443.
9. Hasan RGM, McGuirk JJ. Assessment of turbulence transport models for transonic flow over an axi-symmetric bump. *The Aeronautical Journal* 2001; Paper No. 2562.
10. Durbin PA. Near-wall turbulence closure modelling without 'damping functions'. *Theoretical and Computational Fluid Dynamics* 1991; **3**:1–13.
11. Gatski TB, Speziale CG. On explicit algebraic stress models for complex turbulent flows. *Journal of Fluid Mechanics* 1993; **254**:59–78.
12. Speziale CG, Sarkar S, Gatski TB. Modelling the pressure-strain correlation of turbulence: an invariant dynamical systems approach. *Journal of Fluid Mechanics* 1991; **227**:245–272.
13. Wallin S, Johansson AV. An explicit algebraic Reynolds stress model for incompressible and compressible turbulent flows. *Journal of Fluid Mechanics* 2000; **403**:89–132.

14. Launder BE, Reece GJ, Rodi W. Progress in the development of a Reynolds stress turbulence closure. *Journal of Fluid Mechanics* 1975; **41**:537–566.
15. Johnson DA, Menter FR, Rumsey CL. The status of turbulence modelling for external aerodynamics. *AIAA Paper 94-2226*, 1994.
16. Castro IP, Epik E. Boundary layer development after a separated region. *Journal of Fluid Mechanics* 1998; **374**:91–116.
17. Obi S, Aoki K, Masuda S. Experimental and computational study of turbulent separating flow in an asymmetric plane diffuser. *Proceedings of the 9th Symposium on Turbulent Shear Flows, vol. 3*, Kyoto, Japan, 1993; 305.
18. Buice CU, Eaton JK. Experimental investigation of flow through an asymmetric plane diffuser. *Department of Mechanical Engineering*, *Report No. TSD-107*, Stanford University, U.S.A., 1997.
19. Hellsten A, Rautaheimo P (eds). *Proceedings: 8th ERCOFTAC/IAHC/COST Workshop on Refined Turbulence Modelling*, *Report 127*, 1999.
20. Geurts BJ (ed.). *Modern Simulation Strategies for Turbulent Flow*. Edwards: 2001, ISBN: 1-930217-04-8.
21. Sandham ND. Direct and large eddy simulation. In *Prediction of Turbulent Flows*, Hewitt GF, Vassilicos JC (eds). Cambridge University Press: Cambridge, 2004.
22. Friedrich R, Rodi W (eds). *Advances in LES of Complex Flows*. Kluwer Academic Publishers: Dordrecht, 2002.
23. Geurts BJ, Leonard A. Is LES ready for complex flows? In *Closure Strategies for Turbulent and Transitional Flows*, Launder BE, Sandham ND (eds). Cambridge University Press: Cambridge, 2002.
24. Drikakis D. Advances in turbulent flow computations using high resolution methods. *Progress in Aerospace Sciences* 2003; **39**:405–424.
25. Davidson D, Cokljat D, Frohlich J, Leschziner M, Mellen C, Rodi W (eds). *Large Eddy Simulation of Flow Around a High Lift Airfoil*. Notes on Numerical Fluid Mechanics and Multidisciplinary Design, vol. 83. Springer: Berlin, 2003.
26. Spalart PR, Jou WH, Strelets M, Allmaras SR. Comments on the feasibility of LES for wings and on a hybrid RANS/LES approach. In *Proceedings of the 1st AFOSR Conference on DNS/LES*, Liu C, Liu Z (eds). Greyden Press.
27. Dahlstrom S, Davidson L. Hybrid RANS/LES employing interface condition with turbulent structure. In *Turbulence*, *Heat and Mass Transfer 4*, Hanjalic K, Nagano Y, Tummers M (eds). Begell House, Inc: New York, 2003.
28. Spalart PR. Young person's guide to detached-eddy simulation grids. *NASA/CR-2001-211032*, 2001.
29. Cokljat D, Liu F. DES of turbulent flow over an airfoil at high incidence. *AIAA Paper 002-0590*, 2002.
30. Strelets M. Detached Eddy simulation of massively separated flows. *AIAA Paper 2001-0879*, 2001.
31. Menter FR, Kuntz M, Langtry R. Ten years of industrial experience with the SST turbulence model. In *Turbulence*, *Heat and Mass Transfer 4*, Hanjalic K, Nagano Y, Tummers M (eds). Begell House, Inc: New York, 2003.

